USE OF SATELLITE AND ALS DATA
FOR CLASSIFICATION OF ROOFING MATERIALS
ON THE EXAMPLE OF ASBESTOS ROOF TILE
IDENTIFICATION

Katarzyna Osińska-Skotak, Wojciech Ostrowski

Department of Photogrammetry,
Remote Sensing and Spatial Information Systems
Warsaw University of Technology

A b s t r a c t

Classification of roofing materials with the use of high resolution satellite imagery is a difficult issue, especially due to the fact that roofs are characterised by large diversity of shapes and textures, mainly caused by different roof surfaces illumination. To automate the process of roofing material types classification the influence of diversified illumination of individual roof surfaces should be eliminated. Topographic correction of satellite imagery may decrease influence of such effects and therefore leads to more accurate classification results. This paper presents classification results of roofing materials based on an 8-channel WorldView-2 satellite image. The digital terrain model and the digital surface model created with the use of aerial laser scanning data provided by the ISOK project were used for the topographic correction. The accuracy of the supervised classification of WorldView-2 image achieved for asbestos-cement roofing materials was at the level of 76–92%, (depending on the variant of classification). After grouping roofing materials by similar materials (e.g. painted sheet metal and metal tiles) it is possible to achieve classification results with the accuracy of ca. 70–80%.

Introduction

Classification of very high resolution (VHR) satellite imagery is a challenging issue, especially in case of the pixel-oriented approach. This is due to the high diversity of image texture of various objects, additionally increased by different illumination of individual objects. This effect is visible in multispec-

Correspondence: Katarzyna Osińska-Skotak, Zakład Fotogrametrii, Teledetekcji i Systemów Informacji Przestrzennej, Politechnika Warszawska, pl. Politechniki 1, 00-661 Warszawa, e-mail: k.osinska-skotak@gik.pw.edu.pl

tral images, as well as in pansharpened images. In conventional image classification of roofing material types the diversity of illumination of individual roof surfaces causes the necessity to define multiple training fields for each type of a roofing material. Application of topographic corrections might solve this problem as it limits the illumination variability caused by roof shapes and by the roof position with respect to the Sun at the moment of image acquisition. In order to apply the topographic image correction, data acquired by aerial laser scanning (ALS), available for the majority of Poland, can be utilized to generate a 3D representation of roof surfaces. The topographic correction of satellite imagery can be performed in an automated way. This should potentially contribute to more accurate classification results and to reduction of the workload related to collection of training fields.

The automatic detection of roofing materials has recently become a significant task due to the requirement of removal of all asbestos containing products in Europe by the end of 2032. The restriction on asbestos mining and production, as well as on processing of asbestos containing products in the EU-countries was introduced by the European Parliament and Council Directive 2003/18/WE of March 27, 2003 and the total ban on asbestos use has been introduced by the Directive 1999/77/WE of January 1, 2005. Although asbestos has been mined for several thousand years, its harmfulness for human health has been documented only in the first half of the twentieth century and further classified as a pathogenic and carcinogenic substance. Health problems can occur when asbestos fibres are released into the atmosphere, i.e. during asbestos products deterioration. Due to their small size, when inhaled into respiratory system they are not removed through the usual body purification mechanisms (DYCZEK 2007). Currently deterioration of asbestos-cement products causes the biggest problem for the air pollution additionally accelerated by acid rain and other chemical atmospheric pollutants (SZESZENIA-DĄBROWSKA, SOBALA 2010).

Poland the total marketing suppression on asbestos products has been in force since 1999. According to the Polish asbestos reduction program estimates, in 2008 about 14.5 million tons of asbestos containing products existed („Programme for Asbestos Abatement in Poland 2009–2032"), with majority consisting of flat asbestos-cement plates and corrugated asbestos-cement plates commonly used as roofing materials in sixties and seventies of the 20th century, known under local trade name as Eternit. In accordance with the provisions of „Programme for Asbestos Abatement in Poland 2009–2032" the local government prepares and updates the plan for removal of asbestos and asbestos containing products, based on local asbestos products inventories. According to the information available on the 31st of August 2014 about 80% of municipalities have already completed their inventories (bazaazbestowa.gov.pl). About

4.15 million tons of asbestos containing products were recorded, including 3.97 million tons of asbestos-cement roofing materials. However, only a small fraction (about 205,000 tons) of asbestos containing products has been neutralized till now.

A field inventory is a time consuming process, therefore orthophotomaps from governmental resources are commonly used for asbestos-cement roofing materials inventory. Other image-based materials i.e. VHR satellite images are not used probably due to limited availability, relatively high costs of data acquisition, and in some cases limited spectral resolution.

Remote sensing of roofing materials – literature review

Only a few attempts to utilise aerial or satellite image data for detecting roofing materials have been discussed in literature (HEROLD et al. 2003, ROBERTS, HEROLD 2004, BASSANI et al. 2007). The majority of work consists of urban areas with focus on issues related to automation of classification or building extraction based on object-oriented classification OBIA (e.g. HEROLD et al. 2002, ALMEIDA et al. 2007, CHEN et al. 2009, DINIS et al. 2010). Another direction supplementing urban research is determination of geometric properties of roofs (i.e. BELGIU et al. 2012) and further using such information to determine the function of buildings (VALERO et al. 2008).

A few papers reporting research on remote sensing of roofing materials exist. All of them discuss mostly use of airborne hyperspectral data. HEROLD et al. (2003) dealt with classification of urban areas using data acquired by the AVIRIS hyperspectral scanner recording 224 spectral bands (0.37–2.51 µm), as well as satellite IKONOS and LANDSAT TM data. As reported the classification accuracy based on AVIRIS' 14 spectral channels was dependent on roofing material type (13 material types) and ranged from 40 to 70%. In the case of IKONOS data, the classification accuracy was even lower, mainly due to low spectral resolution. One of the roofing materials, wooden shingle, was classified with a higher accuracy. This result was also confirmed by other work (ROBERTS, HEROLD 2004). The high producer's accuracy was also achieved for ceramic roof tiles, however this class was significantly over-estimated as can be argued from the respective low user's accuracy.

BASSANI et al. (2007) aimed at the detection of asbestos-cement roofing materials by MIVIS hyperspectral scanner (102 spectral channels), ranging from the visible to the far infrared part of the spectrum (0.43 to 2.47 µm and 8 to 14 µm). A detection rate between 80% and 90% could be achieved. MOREOVER, BASSANI et al. (2007) performed detailed spectrometric analyses of asbestos minerals; as a result they confirmed that chrysotile may be detected

in the channel of 2.327 μm. This mineral was mostly used for production of asbestos-cement roofing materials. According to them, another spectral channel, which is interesting for detection of asbestos, is radiation of 9.44 μm wavelength (thermal channel).

Another interesting information on classification of asbestos-cement roofing materials or its properties can be found in the context of inventory and monitoring of urban areas (FONSECA et al. 2011), development and estimation of population in cities (ALMEIDA et al. 2007) as well as, climatic analyses in cities (ATTURO, FIUMI 2005). Overall, the accuracy of asbestos-cement roofing materials classification described in the above mentioned publications was reported as lower than the values achieved by BASSANI et al. (2007).

Methodology

Test field

The test field is the Powsin housing estate, located in the southern part of the capital city of Warsaw (Poland), in Wilanów district. Powsin has been mentioned for the first time in 1259 as the settlement owned by Bogusza Miecławic of the Doliwów family – the voivode of Łęczyca. Since 1951 Powsin has been located inside the administrative boundaries of the capital city of Warsaw. The long history of this area and its rural traditions have had an impact on its current shape. Until now it has preserved a lot of its old character, among others a well preserved street pattern. The majority of buildings in Powsin are single-family houses – detached, semidetached and terraced. The typical for this part of Warsaw farmstead compounds, residential houses with farm buildings, can be found along the main streets. During recent years several estates of single-family houses have been built, mainly as semidetached or terraced houses. Besides single-family houses, a school complex with modern sport fields, the St. Elisabeth of Hungary church and the headquarters of several companies are located in Powsin.

Due to different times of building development various roofing materials can be found at Powsin's area: ceramic tiles, cement tiles, bituminous tiles, metal tiles, different sheet metal, corrugated sheet metal, roofing felt, shingle and asbestos-cement in the form of flat and corrugated plates. The asbestos--cement and the roofing felt are dominant on farm buildings and older houses, the metal tiles on buildings after renovation and the ceramic tiles is the basic roofing material of new, single-family houses (Fig. 1). The metal sheets can be found on farm buildings (painted sheet metal) or on storage sheds and also (the copper sheet) on roofs of several houses and church. As for the shape of roofs,

in the case of the farm buildings mainly flat or gabled roofs can be found while in the case of residential buildings the hip, pyramid hip or multisurface roofs dominate (new single-family detached or semidetached houses). The hip or pyramid hip roofs have slopes between 10º and 15º; most multisurface roofs have slopes between 20º and 35º.

Data source and pre-processing

Threefold data have been used in the study: airborne laser scanning (ALS), the WorldView-2 multispectral satellite image (Fig. 1a) and the roof coverings database (RCDB) (Fig. 1*b*).

The ALS data were acquired for the ISOK Project (IT System of the Country's Protection against Extreme Hazards for Poland, http://www.isok.gov.pl/en/press-releases,press-information-about-isok-project). For the Powsin study area the flight was performed in April 2012 with average point density 12 points/m² (standard II of ISOK Project) obtained from two perpendicular flight paths. Considering the points height accuracy (<0.10 m) of the ISOK standard II data the accuracy of models obtained from these data can be estimated as 15–30 cm (KURCZYŃSKI, BAKUŁA 2013). The ALS data in standard II of ISOK Project were sufficient for modelling the roof planes. Three height models in 0.5 m GRID format were generated with use of the classified point clouds.
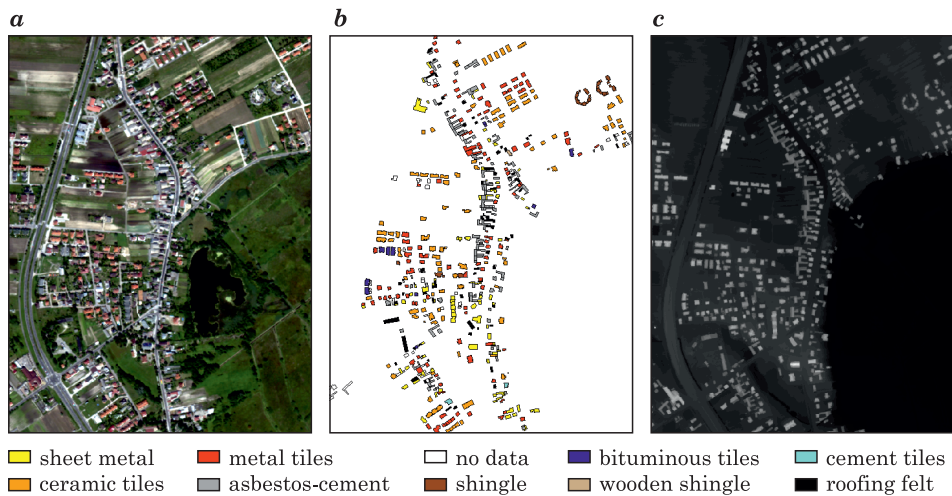

| ☐ sheet metal | ☐ metal tiles | ☐ no data | ☐ bituminous tiles | ☐ cement tiles |
| ☐ ceramic tiles | ☐ asbestos-cement | ☐ shingle | ☐ wooden shingle | ☐ roofing felt |

Fig. 1. Sample of WorldView-2 satellite image (*a*), visualization of the roof coverings database for the study area (*b*) and Digital Surface Model generated based on ALS data (*c*)

The Digital Terrain Model (DTM) was generated based on triangulation of points classified as ground points. During the Digital Surface Model (DSM) generation modelling of the classified point clouds dependent on land cover type according to the rules proposed by HOLLAUS et al. (2010) was applied. To determine the object height in flat (smooth) areas such as ground or roofs the IDW (Inverse Distance Weighting) interpolation was used. For areas covered with medium and high vegetation, considered as rough surfaces, the maximum point height in particular cells of resulting DSM was used (Fig. 1c).

The WorldView-2 image was acquired on August 4, 2011. Multispectral image bands are captured in the following wavelengths: 0.400–0.450 μm, 0.450–0.510 μm, 0.510–0.580 μm, 0.585–0.625 μm, 0.630–0.690 μm, 0.705–0.745 μm, 0.770–0.895 μm, 0.860–1.040 μm. The WorldView-2 satellite does not register middle infrared bands which according to BASSANI et al. (2007) are the most useful spectral range for chrysotile asbestos detection. However, at the start of this study WorldView-2 was the only very high resolution satellite system capturing such a large number of spectral bands, therefore it offered the best possibilities of remote detection of roofing materials. Available satellite systems capturing spectral data at the wavelength of ca. 2.3 μm, that is according to BASSANI et al. (2007) the best wavelength for chrysotile detection, have too large ground sampling distance for detection of roof materials (e.g. OLI on LANDSAT 8, HYPERION on EO-1, ASTER on TERRA). The characteristics of WorldView-2 satellite data used in the study are presented in Table 1.

Table 1

Characteristics of WorldView-2 multispectral image

Acquisition date	2011–08-04
Acquisition time	09:52:16.8
GSD	1.98 m
Global incidence	17.9°
Viewing angle across the track/ viewing angle along the track	17.8°/–1.7°
Sun azimuth	159.7°
Sun elevation	54.0°

The Worldview-2 image orthorectification was performed in the Photomod software (www.racurs.ru) using the Rational Polynomial Coefficients (RPC) model. 21 control points evenly distributed over the test area were used in order to register the scene. Accuracy of the registration was checked with the use of check points (Table 2). The orthorectification was performed in two ways. Firstly, a standard orthophoto with 2 m spatial resolution and a position-

ing accuracy of 2 to 3 pixels was created using the DTM. However, since objects above the terrain appeared displaced and the building roofs included many artefacts, it was decided to use the surface model (including additional information about heights of buildings) in the second orthorectification process. As results improved roofs localization in the corrected image was obtained.

Table 2
Accuracy assessment of orthorectification process of WorldView-2 image (MS DTM orthophoto)

Parameter	dX [px]	dY [px]	ds [m]
Control Points			
	dX [px]	dY[px]	ds [m]
RMS	0.36	0.38	0.28
Mean	0.30	0.30	0.26
Max.	0.57	0.85	0.43
Check Points			
RMS	0.31	0.54	0.31
Mean	0.27	0.48	0.28
Max.	0.42	0.71	0.40

Vector data from the roof covering database (RCDB) were used as the reference data for the classification accuracy assessment. This database was created based on visual interpretation of aerial orthophotomaps (with ground resolution of 0.25 m, building boundaries at ground level) and on the field observations. There are 636 residential houses and farm buildings in the roof covering database of Powsin housing estate.

Experiments description

In order to evaluate the possibilities of automatic extraction of information on roofing material types several experiments were performed which included the supervised classification. All operations were performed with the use of ERDAS Imagine 2014 software, made available by the Intergraph Polska. The flowchart of the procedure used in the study is shown in Figure 2, where MS stands for multispectral image, MS DTM for standard orthophoto based on the DTM, MS DSM for true-orthophoto based on the DSM and MS TOPO for true-orthophoto based on the DSM and with topographically corrected roof reflectance's. The superscript „f" indicates results after majority filtering.
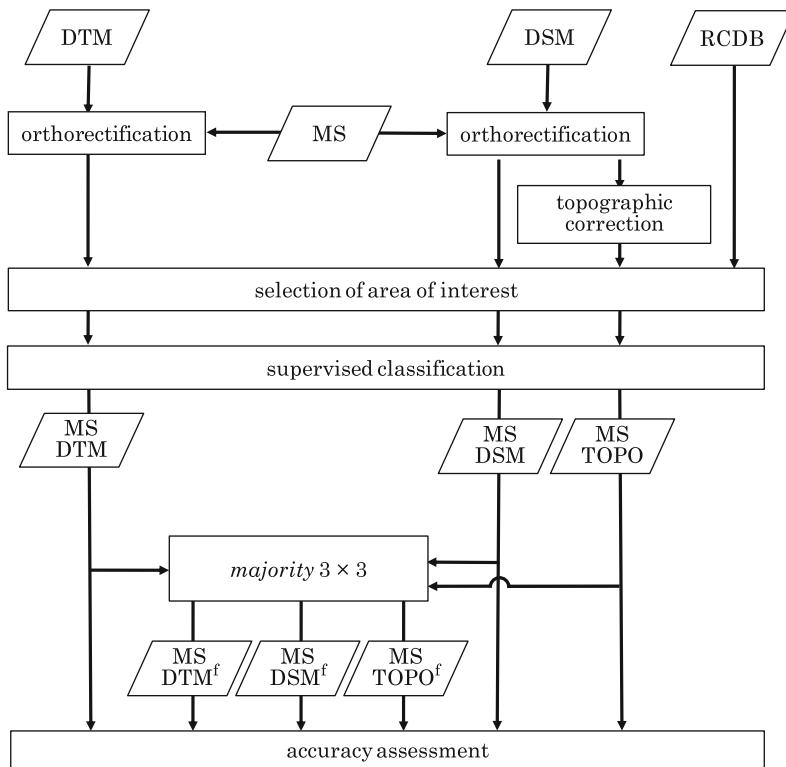
Fig. 2. Methodology scheme

The supervised classification was performed for the building roofs only, obtained by masking areas outside of the roof coverings vectors (RCDB). Building outlines could also be obtained from laser scanning data by applying an appropriate filtering algorithm. In many cases the ALS-based roofs and those from the RCDB overlap and in deliver comparatively satisfying results, but especially in regions with tall vegetation hanging OVER roofs problems occur. Therefore the decision has been made to further use the RCDB only.

The supervised classification was performed using the maximum likelihood algorithm for set of orthophotos: the MS DTM, the MS DSM, and the MS TOPO. Topographic effect is caused by differences in illumination due to the incidence angle of sun radiation onto the object surface, thus a significant variation in the pixel values of the same object occurs. One way to reduce topographic effect in imagery is by applying transformations based on the Lambertian reflectance models. The topographic corrections were performed with the cosine method described, among others, in RICHTER et al. (2009). This

method assumes that the surface reflects incident solar energy uniformly in all directions, and that variations in reflectance are due to the amount of incident radiation which in turn depends on the incidence angle of the illumination (COLBY 1991). But for low illumination, i.e., large incidence angles and thus small values of cosine, the corrected reflectance is too large and the corresponding parts of an image are overcorrected (RICHTER et al. 2009). In the study area in most cases the local solar illumination angles vary in the range of 15–58°. The largest angles of incidence are on the north-west facing roof planes because of the south-east sun azimuth at the time of image acquisition.

For every variant a set of training fields was prepared, representing all types of roofing materials present within the study area, namely: sheet metal, metal tiles, bituminous tiles, cement tiles, ceramic tiles, asbestos cement, shingle, wooden shingle (only one roof) and roofing felt. In the case of the sheet metal roofings three training fields (zinc coated sheet metal, copper sheet and painted sheet – only red painted sheet in the study area) and for metal tiles two training fields (red metal tiles and dark red metal tiles) were defined. Prepared training fields contain ca. 300–500 pixels. Examples of spectral characteristics of class patterns obtained for multispectral image (MS DSM orthophoto) are presented in Figure 3.
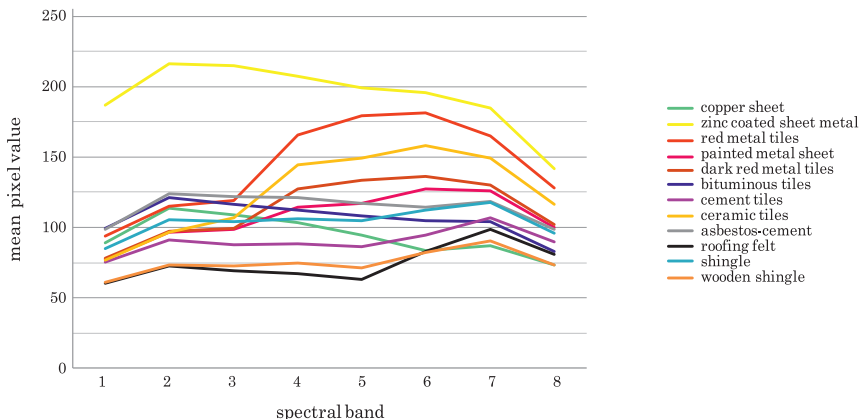

Fig. 3. Mean spectral characteristics of class patterns obtained for MS DSM orthophoto

Due to the spatial resolution of 2 m the stripe texture of roofing materials for corrugated metal plates and asbestos-cement plates, often used as roofing material of farm buildings, was not visible. This limited the necessity to define more samples and simplified the process of representative sample selection. All training fields fulfilled the criteria for this type of patterns. The evaluation of class separability with the transformed divergence and Jeffries-Mattusita's

distance yielded good results, except for the following pairs: dark red metal tiles and ceramic tiles, asbestos-cement and cement tiles, asbestos-cement and shingle (cement shingle), shingle and copper sheet as well as dark red metal tiles and red painted sheet. The latter pair showed the highest radiometric similarity and therefore it was decided not to include the red painted sheet in the classification process. When analysing the separability of training fields derived from the three variants of input data (i.e. MS DTM, MS DSM, MS TOPO), MS TOPO showed a slightly better separability than MS DSM.

Results analysis and discussion

The obtained classification results show that roofs made of one material are usually classified as several types of roofing materials (Fig. 4). That effect is mainly caused by the differences in illumination of individual roof shapes caused by additional roof elements such as skylights, roof windows, chimneys, and so-called the mixels on roof edges.

The variable influence of illumination is clearly visible in the case of classification of the multispectral image after orthorectification with the use of DTM (MS DTM, Fig. 4*a*) as well as after orthorectification with the use of DSM (MS DSM, Fig. 4*b*). The satellite image was acquired at 9:52 AM and with the south-east Sun position the north-west roof shapes were half-shaded. After detailed analysis of obtained results it can be noticed that after orthorectification with the use of DSM the number of mixels on roof edges decreased, but it has no significant influence on evaluation of classification results. Unfortunately, the topographic correction performed with the cosine method did not result in expected significant improvement of the classification results. An improvement is only visible in the case of roofs with not complicated shapes with a relatively low slope angle value. In the case of multi-shaped roofs of diverse slopes the topographic correction resulted in deterioration of the classification results. The main problem concerning topographic correction is that the cosine method results are overcorrected for low illumination (RICHTER et al. 2009). In the case of areas with diversified relief or roofing shapes this type of situations occurs quite often (in the analysed image it may be visible only on the northern-west side of roofs).

Due to the fact that several classes can be found in an individual roof, including single-pixel classes, a *majority* 3×3 filter was used to filter the classification results. This filter selects the most common pixel value within the filter window. In result more homogeneous classification results were obtained for individual roofs and the influence of edge-pixels and pixels of different roof elements (such as roof windows, roof hatches, chimneys) was limited. The result after filtering is presented in Figure 4*d, e, f*.
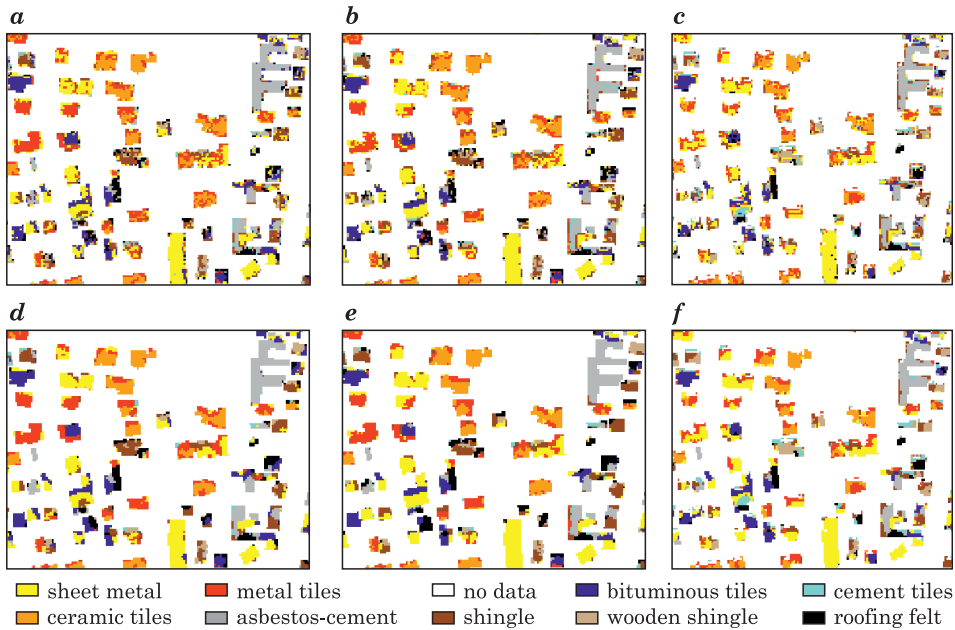
Fig. 4. Comparison of the supervised classification results of the multispectral image orthorectified using the DTM (*a*), the multispectral image orthorectified using the DSM (*b*), the multispectral image orthorectified using the DSM after topographic correction (*c*) and results of classification after majority filter 3×3 (*d*, *e*, *f*)

Evaluation of the classification results was done by comparison with the roofing materials coverings database. It was performed according to two approaches: a conventional pixel-oriented and the object-oriented approach[1], with respect to the roofing materials vector database. In the per object analysis for individual roof (polygon/object in vector database) major roofing material type is considered because during the field survey it was not noticed that the mixed type of roofing material for individual building existed. Additionally it eliminates the problem of different class values in the case of edge pixels or pixels of roof windows or pixels of different elements of roofs which results in incorrect values of roofing material classes.

Comparison of the classification results of different input data given per object with the reference database is presented in Figure 5. Results obtained from classification of three orthophotos (MS DTM, MS DSM, MS TOPO) seem to be similar when compared visually however some differences rise in the accuracy assessment statistic. Table 3 presents results of the accuracy assessment of several classification variants, according to the pixel and per object approaches, for: MS DTM, MS DSM, MS TOPO.

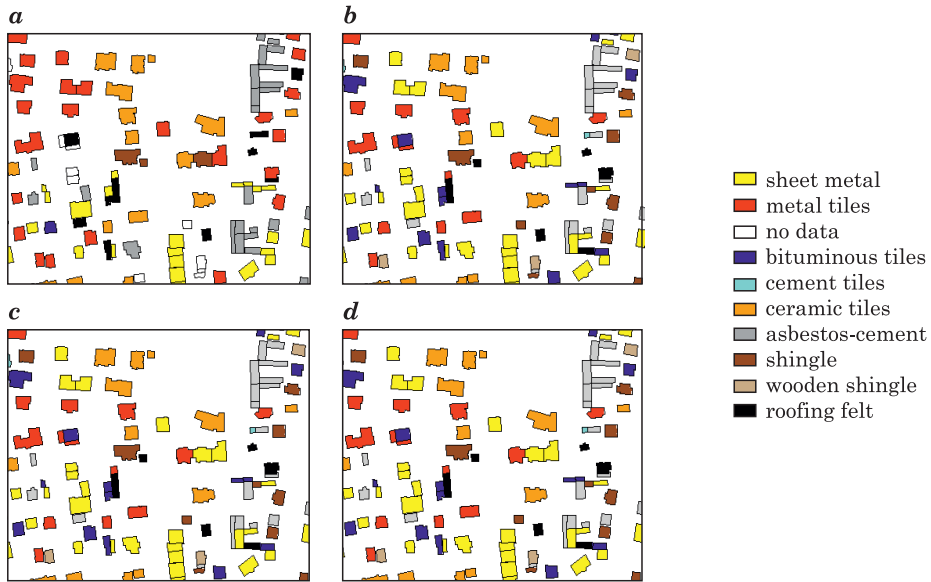[1] Not to be confused with of object oriented classification (OBIA).

Fig. 5. Comparison of supervised classification results in object-oriented approach of the multispectral image orthorectified using the DTM (*b*), the multispectral image orthorectified using the DSM (*c*), the multispectral image orthorectified using the DSM after topographic correction (*b*), and the roofing materials database (*a*)

Based on results analysis it may be stated that asbestos-cement roofing, as well as ceramic roofing plates are classified with the highest accuracy. In the case of other roofing materials both, much lower producer's and user's accuracy may be noticed. For the asbestos-cement roofing and ceramic roofing plates slightly higher values of the user's accuracy may be noticed for the image orthorectified based on the DSM than with the use of the DTM. This results from the fact that in an image rectified based on the DSM the roof position is correct (no building layover effect) and after masking of the area of interest we deal with the lower number of edge pixels.

In the case of information extraction concerning asbestos-cement roofing the producer's accuracy reaches the level of 81–85%, depending on the type of classified data. The user's accuracy reaches 57–66% in this case. Asbestos-cement roofings are quite often classified as (damaged) roofing felt or cement roof tiles or cement shingle. In the case of ceramic roof tiles the producer's accuracy reaches as much as 95%, but the user's accuracy varies between 41 and 53%. This is due to the fact that roofs with red metal roof tiles are mainly classified as ceramic roof tiles. Similar accuracy was obtained by HEROLD et al. (2003) for classification of ceramic roof tiles. However, using the principle component analysis method (made only for roofs image), at the stage

Table 3

Summary of the accuracy* of different variants of the classification – the pixel-oriented approach (P) and pre object (O). MS DTM – multispectral image orthorectified using the digital terrain model, MS DSM – multispectral image, orthorectified using the digital surface model, MS TOPO – multispectral image after orthorectification using the digital surface model after topographic correction

Specyfication		Sheet metal	Metal tiles	Bituminous tiles	Cement tiles	Ceramic tiles	Asbestos-cement	Shingle	Roofing felt
Validation samples — No. of pixels		54715	87852	11112	2324	99546	**77968**	13673	42935
No. of roofs		83	120	11	4	101	**143**	26	82
MS DTM user's accuracy	P	54.4	29.3	45.3	40.7	50.0	**65.7**	33.4	28.6
	O	63.9	34.2	45.5	50.0	57.4	**79.7**	42.3	39.0
producer's accuracy	P	43.9	36.0	11.7	6.4	94.5	**81.5**	11.0	52.8
	O	53.0	47.1	8.1	5.9	100	**86.4**	20.4	71.1
MS DSM user's accuracy	P	56.8	26.6	41.5	42.8	52.6	**65.8**	35.2	30.5
	O	65.1	26.7	27.3	50.0	59.4	**84.2**	46.2	40.2
producer's accuracy	P	46.2	35.9	13.0	6.0	93.7	**81.3**	10.3	48.4
	O	58.1	42.1	6.3	5.0	98.4	**88.1**	16.4	64.7
MS TOPO user's accuracy	P	51.9	21.6	40.4	41.7	41.1	**57.1**	26.7	25.5
	O	59.0	20.8	45.5	50.0	47.5	**76.9**	23.1	20.7
producer's accuracy	P	34.5	29.8	11.7	4.0	89.0	**84.6**	9.4	58.9
	O	44.5	37.3	7.4	2.9	98.0	**91.7**	10.9	58.6
MS DTM** user's accuracy	P	57.8	32.0	51.0	53.1	52.4	**74.1**	41.2	31.9
	O	61.4	33.3	45.5	50.0	56.4	**79.7**	42.3	36.6
producer's accuracy	P	49.6	37.0	13.1	10.1	97.3	**85.1**	15.1	56.5
	O	53.7	46.5	8.3	6.3	100	**86.4**	17.5	71.4
MS DSM** user's accuracy	P	60.5	27.9	46.7	56.3	56.2	**73.9**	40.9	35.7
	O	66.3	26.7	27.3	50.0	59.4	**83.9**	46.2	42.7
producer's accuracy	P	52.1	36.6	14.6	9.3	96.3	**84.9**	13.2	51.7
	O	60.4	41.6	6.7	5.3	98.4	**88.2**	16.7	66.0
MS TOPO** user's accuracy	P	56.4	22.1	48.3	47.2	45.5	**65.6**	28.7	26.4
	O	57.8	20.8	45.5	50.0	47.5	**76.2**	26.9	23.2
producer's accuracy	P	39.4	30.9	13.4	4.6	94.4	**87.4**	11.2	62.5
	O	46.2	35.2	7.7	2.4	96.0	**91.6**	13.2	67.9

* – because in the test area there is only one building with wooden shingle, it was omitted in the accuracy assessment.
** – image after filtering using *majority* 3×3 filter.

prior to the image classification, it is possible to improve the classification accuracy of those roofing materials (the user's accuracy may be improved to 70%). This was proved by (OSIŃSKA-SKOTAK 2014).

For the assessment per object higher accuracy was achieved for all types of roofing materials, both, with respect to the user's and the producer's accuracy. The highest accuracy was obtained for asbestos-cement roofing materials. In the case of classification of an image after topographic rectification accuracy of almost 92% was obtained, and the user's accuracy reached 77%. Image filtering using the *majority* 3×3 filter did not lead to considerable improvements in obtained accuracy.

When analysing the list of results presented above, it may be noticed, that the applied topographic correction did not considerably improve the classification results. Only improvements of the classification results may be seen in the case of uncomplicated, gable or hip pyramid roofs or in the case of hip roofs. In the case of more complicated roof constructions of high inclination angles, too high „saturation" value of pixels is noticeable. This might be partly explained by differences in spatial information content between satellite multispectral data (2 meters) and ALS data used.

Conclusions

Results of experiments performed in the study prove that automatic detection of roofing materials is a challenging issue. The highest accuracy of the supervised classification of the WorldView-2 image was achieved for asbestos--cement roofing materials (76–92%, depending on the variant of classification). Another type of roofing materials which is characterised by the very high producer's accuracy are ceramic roof tiles. Much lower accuracy values were achieved for other types of roofing materials. This results from the high similarity of some roofing materials (metal tiles, painted steel plates, bituminous tiles and roofing felt). However, after grouping roofs made of similar materials it is possible to achieve classification results with the accuracy of ca. 70–80%.

As presented, the accuracy of classification of a multispectral image orthorectified with the use of the digital surface model is slightly higher comparing to the accuracy of classification of a multispectral image orthorectified using the digital terrain model. Unfortunately, topographic correction of a multispectral image performed using the cosine method did not result in expected improvements of roofing materials classification results. Some positive effects may be seen only in the case of uncomplicated roof construction, such as gable and hip pyramid roofs, as well as hip roofs.

Acknowledgements

References

ALMEIDA C.M., SOUZA I.M.E., ALVES C.D., PINHO C.M.D., PEREIRA M.N., FEITOSA R.Q. 2007. *Multilevel Object-Oriented Classification of QuickBird Images for Urban Population Estimates*. 15th ACM International Symposium on Advances in Geographic Information Systems (ACM GIS 2007), Seattle.

ATTURO C., FIUMI L. 2005. *Thermographic analyses for monitoring urban areas in Rome to study Heat Islands*. International Conference „Passive and Low Energy Cooling 145 for the Built Environment", May' 2005, Santorini, Greece, p. 145–150.

BASSANI C., CAVALLI R.M., CAVALCANTE F., CUOMO V., PALOMBO A., PASCUCCI S., PIGNATTI S. 2007. *Deterioration status of asbestos-cement roofing sheets assessed by analyzing hyperspectral data*. Remote Sensing of Environment, 109(2007): 361–378.

BELGIU M., TOMLJENOVIC I., LAMPOLTSHAMMER T.J., BLASCHKE T., HÖFLE B. 2012. *Ontology-Based Classification of Building Types Detected from Airborne Laser Scanning Data*. Remote Sensing, 6: 1347–1366, DOI:10.3390/RS6021347.

CHEN Y., SU W., LI J., SUN Z. 2009. *Hierarchical object-oriented classification using very high resolution imagery and LIDAR data over urban areas*. Advances in Space Research, 43: 1101–1110.

COLBY J.D. 1991. *Topographic Normalization in Rugged Terrain*. Photogrammetric Engineering & Remote Sensing, 57(5): 531–537.

DINIS J., NAVARRO A., SOARES F., SANTOS T., FREIRE S., FONSECA A., AFONSO N., TENEDÓRIO J. 2010. *Hierarchical object-based classification of dense urban areas by integrating high spatial resolution satellite images and LIDAR elevation data*. The International Archives of the Photogrammetry, Remote Sensing and Spatial Information Sciences, XXXVIII(4/C7): 6.

DYCZEK J. 2007. *Azbest i materiały zawierające azbest. Ocena ryzyka emisji włókien azbestu*. In: *Bezpieczne postępowanie z azbestem i materiałami zawierającymi azbest*. Ed. J. Dyczek. Wydawnictwo Naukowe „Akapit", Kraków, p. 7–26.

FONSECA L., NAMIKAWA L., CASTEJON E., CARVALHO L., PINHO C., PAGAMISSE A. 2011. *Image Fusion for Remote Sensing Applications*. In: *Image Fusion*. Ed. O. Ukimura. Publisher: InTech, p. 153–178.

HEROLD M., SCEPAN J., MÜLLER A., GÜNTHER S. 2002. *Object-Oriented Mapping and Analysis of Urban Land Use/Cover Using IKONOS Data*. Proceedings of 22nd EARSeL Symposium Geoinformation for European-Wide Integration, Prague, Czech Republic, 4–6 June 2002.

HEROLD M., GARDNER M., ROBERTS D. 2003. *Spectral resolution requirements for mapping urban areas*. IEEE Trans. Geoscience Remote Sensing, 419): 1907–1919.

HOLLAUS M., MANDLBURGER G., PFEIFER N., MÜCKE W. 2010. *Land cover dependent derivation of digital surface models from airborne laser scanning data*. The International Archives of the Photogrammetry, Remote Sensing and Spatial Information Sciences, 38: 1–3.

KURCZYŃSKI Z., BAKUŁA K. 2013. *The selection of aerial laser scanning parameters for country wide digital elevation model creation*. 13th SGEM GeoConference on Informatics, Geoinformatics and Remote Sensing. SGEM2013 Conference Proceedings, 2: 695–702, DOI:10.5593/SGEM2013/BB2.V2/S10.020.

OSIŃSKA-SKOTAK K. 2014. *Zastosowanie technik teledetekcyjnych do inwentaryzacji cementowo-azbestowych pokryć dachowych*. Teledetekcja Środowiska, 51(2): 73–83.

RICHTER R., KELLENBERGER T., KAUFMANN H. 2009. *Comparison of topographic correction methods.* Remote Sensing, 1: 184–196, DOI:10.3390/RS1030184.

ROBERTS D.A., HEROLD M. 2004. *Imaging spectrometry of urban materials.* In: *Infrared Spectroscopy in Geochemistry, Exploration and Remote Sensing.* Eds. P. King,, M.S. Ramsey, G. Swayze. The Mineralogical Association of Canada, Short Course Series, 33: 155–181.

STORY M., CONGALTON R. G. 1986. *Accuracy assessment: A user;s perspective.* Photogrammetric Engineering and Remote Sensing, 52: 397–399.

SZESZENIA-DĄBROWSKA N., SOBALA W. 2010. *Zanieczyszczenie środowiska azbestem. Skutki zdrowotne.* Raport z badań, Instytut Medycyny Pracy im. prof. J. Nofera, Oficyna Wydawnicza MA, Łódź.

VALERO S., CHANUSSOT C., GUEGUEN P. 2008. *Classification of basic roof types based on VHR optical data and digital elevation model.* IGARSS' 2008, Commission IV, p. 149–152.